Energy Reports 8 (2022) 5329–5340

Contents lists available at ScienceDirect

Energy Reports

journal homepage: www.elsevier.com/locate/egyr

Research paper

Influence of the type of solar protection on thermal and light performance in classrooms

Cristián Muñoz-Viveros [a,b], Alexis Pérez-Fargallo [c,*], Carlos Rubio-Bellido [d]

[a] Center for Research in Construction Technologies (CITEC), University of Bío-Bío, Concepción, Chile
[b] Department of Theory and Design, Faculty of Architecture, Construction, and Design, University of Bío-Bío, Concepción, Chile
[c] Department of Construction Science, Faculty of Architecture, Construction, and Design, University of Bío-Bío, Concepción, Chile
[d] Department of Building Construction II, University of Seville, 41012, Seville, Spain

ARTICLE INFO

Article history:
Received 8 February 2022
Received in revised form 28 March 2022
Accepted 5 April 2022
Available online xxxx

Keywords:
Energy optimization
Passive architecture
Solar protection
Classrooms

ABSTRACT

Solar protections are often designed as passive strategies in buildings, both for thermal and lighting performance. In this sense, the importance of the balance between these two parameters could be crucial in the early stages of design. The purpose of this research is to compare the variation solar protection strategies (glazing with solar protection, and the length of overhangs) have on energy and lighting, using as reference, the value defined by the Modified Solar Factor (MSF), used in some countries like Spain and Chile, to restrict solar contributions. Simulations were carried out to understand the potential of solar protections with the same MSF and the implications on thermal and lighting performance. The case study is a classroom located in Talca, in central-southern Chile, with a climate of marked seasons, including cold winters and hot summers. The results showed that the use of solar protection strategies with the same and similar MSF values do not provide comparable energy performance. Specifically, the differences in energy consumption are 0.62 kWh (East (E) - MSF 0.14) for heating, in cooling 42.28 kWh (Northeast (NE) - MSF 0.47), in lighting 5.30 kWh (Northwest (NW) - MSF 0.11), and 39.77 kWh in the total consumption (Northeast (NE) - MSF 0.47). According to the results obtained, suitable solar protection requires evaluating different alternatives that allow balancing both performances, while attaining significant energy savings.

1. Introduction

The impact that early design strategies for the façade have on the energy needs of a building and the comfort of their occupants, can reach up to 20% in the following stages, and up to 80% for all other design decisions (Vullo et al., 2018). This impact depends on the availability of local solar radiation, the geometry of openings, their wall percentage, the orientation, devices, characteristics of the materials, among others, and determining the daylighting levels of the premises and the thermal losses or gains these have through the envelope. In addition, the geometry, size, and distribution of the opening (Larrumbide and Bedoya, 2015), the optic characteristics (light transmittance of the glazed surfaces), and the behavior of energy passing through (transmission, absorption, and refraction), can have a positive or negative effect (Lee et al., 2013). For this reason, lighting and thermal requirements are contrasted against one another, as in given climates, large glazed surfaces can contribute suitable levels of thermal comfort, but not visual, and vice versa (Bustamante et al., 2012; Correia da Silva et al., 2013). As a result, acknowledging local conditions leads to the definition of more suitable strategies (Tzikopoulos et al., 2005), considering the multiple requirements to ensure visual comfort (Ochoa et al., 2012) and, in some cases, establishing recommendations in different climates. This has been seen in different studies that address the problems of saving energy and the impact of early design decisions on multivariable performance to make contrasting demands compatible, and achieving an optimal balance between energy contributions for heating–cooling and the daylight needs in office buildings, schools, and homes (Al-Khatatbeh and Ma'Bdeh, 2017; Lee et al., 2013). The validation of contrasting hypotheses has been resolved through simulations (Lee et al., 2013), monitoring campaigns, or real-scale assessment, trying to balance both requirements (Tsikra and Andreou, 2017), finding partial increases in energy consumption, but reductions in overall consumption (Boafo et al., 2019). On the other hand, solar control experiences have been carried out, which restrict the optical properties of the glass (Alhagla et al., 2019; Huang et al., 2014), the thermal transmittance value, or the window-to-wall ratio, among other parameters (Alwetaishi and Taki, 2020; Bodart and De Herde, 2002; Goia et al., 2013).

As a result, some researchers indicate that the search for metrics or indicators, which include the dynamic of seasonal and

* Corresponding author.
E-mail address: aperezf@ubiobio.cl (A. Pérez-Fargallo).

https://doi.org/10.1016/j.egyr.2022.04.007

Nomenclature and abbreviations

Con	Thermal conductivity
CITEC-UBB	Center for Research in Construction Technologies - University of Bío-Bío
DB	DesignBuilder Software
DECON-UC	División Escuela de Construcción-Pontificia Universidad Católica de Chile (School of Construction Division - Pontifical Catholic University of Chile)
emis	Emissivity
IRT	Infrared Transmission Factor
LBNL	Lawrence Berkeley National Laboratory
Minvu	Ministerio de Vivienda *y* Urbanismo (Ministry of Housing and Urbanism)
MSF	Modified Solar Factor
NCh	Norma Chilena (Chilean Standard)
N	North
NE	Northeast
NW	Northwest
S	South
ST	Solar Transmission Factor
SR	Solar Reflectance Factor
VT	Visible Transmission Factor
VR	Visible Reflectance Factor.
W	West

climate variability, could obtain spaces that better fit the user's biological and psychological needs, acknowledging local conditions and the use of spaces (Acosta et al., 2016; Carlucci et al., 2015). For this reason, the study of lighting addressed as a static problem, evolved on including indicators that combine time and space, assuming the dynamic issue of solar behavior and seasonal variation together with other variables such as outdoor views and areas with direct sunlight, which are understood as part of a better perception of visual comfort (Carlucci et al., 2015; Pellegrino et al., 2015). Therefore, the multi-objective method for openings design is presented as a challenge (Ashrafian and Moazzen, 2019; Shan, 2014), but would allow for early approaches to decision-making in the project (Lartigue et al., 2014; Ochoa and Capeluto, 2009; Østergård et al., 2016; Shahbazi et al., 2019), ensuring relevant energy reductions in the operation stage, and optimizing the construction process at the same time. In addition, by showing shading parameters and daylight indicators, it is possible to define geometries and study suitable layouts, playing an important role in the image and identity of the building (Xue et al., 2019). In this sense, multi-variable methodologies have been used that address energy (heating and/or cooling) and energy consumption or lighting performance issues, whether thermal or lighting and thermal or visual comfort (Chi et al., 2018; Kwon and Lee, 2018), exploring passive strategies based on the design of solar protections that play a double role: avoiding the entry of excess solar radiation and regulating the entry of daylight (Carlos, 2017; Uribe et al., 2019). The development of these methodologies has focused on using different calculation proposals such as genetic algorithm models (Jalali et al., 2020; Zhai et al., 2019), and parametric modeling techniques (Fang and Cho, 2019), which have led to formal results with atypical shading solutions (Kirimtat et al., 2019). In addition, results have been sought using statistical techniques through sensitivity analysis that consider different scenarios (Shaeri et al., 2019; Wang et al., 2020; Xue et al., 2019; Zhang et al., 2017) and, innovative methodologies have been assessed, such as pixel counting (PxC) in the videogame area, enabling approaches to assess complex shading devices using incident light on indoor surfaces, and the impact of complex parametric shading systems (de Almeida Rocha et al., 2020). Other research has also evaluated using other methods such as Computational Fluid Dynamics (CFD) which has allowed having more accurate evaluations of the behavior of building typologies with large glazed surfaces, reporting significant savings in lighting and total energy (Cheong et al., 2020).

As it can be seen, energy-saving strategies tend to be focused on solving problems of the thermal envelope and its limitations on energy transfer, avoiding excessive losses or gains, which is reflected in the updates included in the standards and regulations (Dirección General de Arquitectura, 1998; Gasparella et al., 2011; MINVU, 2017). However, despite progress in multi-objective methodologies, standards still depend on metrics that favor or worsen one over another, leading to unsuitable combined solar protection and natural lighting strategies, which have considerable rises in energy demand when compared to an optimized case (Ochoa and Capeluto, 2009). In this sense, one approach to solar protection demands is by using indicators that consider thermal aspects based on the optical properties of their opening's elements, such as the Modified Solar Factor (MSF), applied by the Spanish Technical Building Code (Dirección General de Arquitectura, 1998) or the Standardized Terms of Reference in Chile (CITEC-UBB, DECON-UC, Dirección de Arquitectura, 2015). The MSF is a ratio between the characteristics of the opening and the amount of solar radiation that this absorbs, reflects, and transmits into the premises. An unobstructed opening would have an MSF equal to 1, and the incorporation of elements will reduce this value on intervening between the available local solar radiation and the indoor space. This acknowledges that the greatest impact on energy performance from an opening, is the light transmission factor and the total solar energy or solar factor (g) transmission factor (INE, 1997; UNE-EN, 2011), one duly offsetting the other (Simmler and Binder, 2008). Currently, it is possible to reach similar MSFs with different types of solar protections such as overhangs, latticework, setbacks, and solar control glazing, and obtain similar behavior patterns on comparing cooling and heating demands (Ahmad et al., 2021). However, it does not consider that the type of protection has a dynamic behavior throughout the year and, thus, despite efforts to consider multi-objective methodology in early design stages, there is no research that shows the impact on contrasting performances on using different solar protections with a similar MSF on energy consumption parameters (heating, cooling, and lighting). For this reason, this article has the purpose of analyzing the differences in using solar protection through the Solar Transmittance (ST) of the glazed surface versus solar protection via overhangs, evaluating the energy consumption of heating, cooling, and lighting, and the differences there may be, even when both have equal values defined by the MSF numerical calculation.

2. Methodology

The research methodology was organized in 5 stages (Fig. 1). Stage 1 determined the MSF, by numerical calculation, using different dimensions for the depth of overhangs defined in the location and orientation being assessed. Stage 2 generated energy simulation models in DesignBuilder, setting their solar protection variables. Stage 3 made the energy simulations and the results collection process associated with both solar protection strategies (overhang and setback). Stage 4 analyzed and compared the results. Stage 5 performed the sensitivity analysis of variables using R-statistic software, to evaluate the impact of the main parameters used.

The experiment was run in Talca, Chile, which has a marked seasonal variability, analyzing the thermal and light behavior in a standard school classroom over one year.

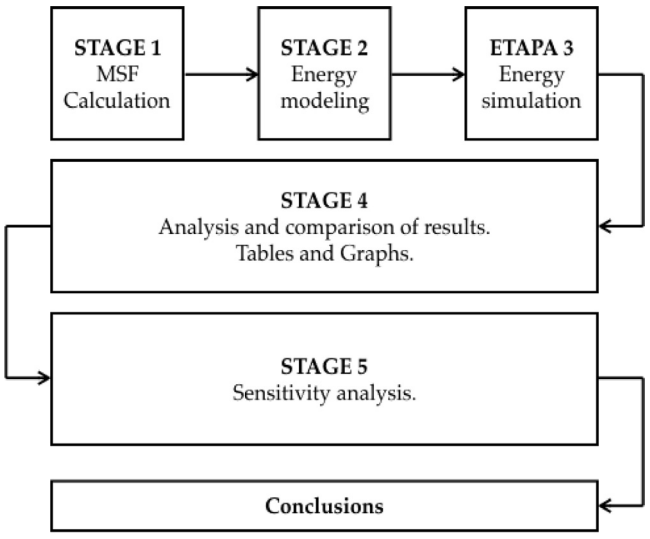

Fig. 1. Process and analysis tools.

2.1. Base case

A school classroom of 9.00 × 6.00 × 3.00 m was used, with 20 cm thick reinforced concrete walls, and a three-section window on one of its façades: one of 1.60 × 1.40 m, and two of 1.60 × 2.80 m. It has a 0.90 m sill, measured inwards, and 20 cm separations between the glazed surfaces, for the pillars. The windowed façade faces outside and defines the orientation of the model. The other faces of the model are considered adiabatic. The characteristics of the premises and its dimensions are shown in Fig. 2.

The formula established in the HE Basic Document of the Spanish Technical Building Code is used as a reference to determine the MSF and the tables that link the dimensions of the opening and the solar protection elements. For this case, the table established for the overhang and setback elements has been used (Table 1). The MSF can be described as follows:

$$MSF = SF \cdot [(1 - F_v) \cdot g\perp + FF \cdot 0,04 \cdot UF \cdot \propto] \quad (1)$$

where F is el MSF, SF is the shading factor, F_v is the fraction of the hollow space occupied by the glass, $g\perp$ is the solar factor of the glass (UNE EN 410:1988), FF is the fraction of the hollow space occupied by the frame, UF is the transmittance of the frame (W/m^2 K) and $\propto$ is the absorptance, considering the window frame's color.

To obtain the value for the geometry of the case study's glazed surface, variations for solar protection with overhangs of 10 to 400 cm in depth were used, with single glazing, and the following frame colors: half white in aluminum with thermal bridge break for the North, Northeast, Northwest, East, and West orientations. To determine the characteristics of the case study's envelope, those defined in the Energy Efficiency Guide for Educational Establishments of the Chilean Energy Efficiency Agency were used (2012).

2.2. Simulation and boundary conditions

The climate file of the location under evaluation was obtained using the Meteonorm v.7.0 software, considering the official station suggested by it. To determine the hours of sunshine (Wh/m^2 × day), the data of the Chilean Standard 1079 Of. 2008 and the Climate Consultant v 6.0 software are used, as well as the EPW file obtained for values not found in the Standard. The qualitative values and appreciation, according to NCh 1079 for the average temperature, are 20.3 °C (Very high - very hot) in January, and 7.6 °C (Low - cold) in July. The monthly mean oscillation for January is 18.9 °C (Mean), and for July, 11.4 °C (Mean). Sunlight in January is 6445 Wh (m^2 × day) (Strong) and in July, 926 Wh (m^2 × day) (Very low).

Occupation periods are established for the classroom, from Monday to Friday, between 8 am and 6 pm, with an occupation of 27 people, and an infiltration of 0.7 air changes per hour (ac/h), for one year, without discounting winter and summer vacations. An operation is considered for the lighting systems, when 400 lux, 0.8 m above the work plane is required, with an on/off system (see Table 2).

Walls, floor, and a reinforced concrete cover without an adiabatic covering are set for the classroom envelope, except for the windowed wall, which has a 60 mm thick expanded polystyrene thermal insulation with a U value of 0.59 W/m^2 K established by the local standards.

The DesignBuilder (DB) energy simulation program uses the EnergyPlus calculation engine. This allows modeling the geometries of complex openings, and efficiently including boundary conditions and the modification of the overhang and glazing parameters, thus covering the entire range of possible values, applying the numerical ratios indicated in Table 1.

For glazed surfaces, MSF values are defined using calculations for the overhang and its equivalent, in a 0.1 m deep setback. The values for overhangs are separated into 4 ranges: 0.1 to 0.8 m; 0.9 to 1.6 m; 1.7 to 3.2 m; and 3.3 to 4.0 m. These ranges establish values that vary for the N, E–W, and N–N orientations.

The g value of the glazing is established from these values, for its equivalent in cases without overhangs. In this way, the optical characteristics of the glazing are defined from the databases of DB and the LBNL Window software, for each level of solar protection. An overhang with single glazing, with an ST of 0.82, is set for the simulations. The optical characteristics of the glazing are presented in Table 3.

With the MSF values of the combinations determined from the calculations, these are input in the DB model to obtain heating/cooling and lighting energy consumption values. This is repeated for each defined MSF and ST combination. With the overhang, this is evaluated with ST 0.82 and overhang dimensions of between 0.1 and 4.0 m for the defined orientations (N, NE, NW, E, and W). This allows comparing the values obtained and, later, determining the impact that using one strategy or the other has on the final energy demand.

R Studio software was used to determine statistical values associated with the results obtained, considering the total energy data and their dependence on the Solar Transmittance values of the glazing (ST) and the overhang depth. Once the energy simulation results were obtained, the data was entered into R Studio to run a sensitivity analysis, considering the variables of the orientation, glazing type, and solar protection system: overhang or solar transmission factor of the glazed surfaces. A p-value of 0.05 was considered as an indicator of significance for the variables.

3. Results and discussion

3.1. Obtaining properties for solar protections

By applying the MSF formula, it is possible to determine the value associated with each overhang length, considering other preset parameters for the geometry of the opening, and the values associated with this (frame type, color, glazing type) (Table 4). For overhang depths between 0.1 and 4.0 m, a curve was obtained that is arranged by sections, where the MSF is considered as constant, obtaining variations at 0.9 m, 1.7 m, and 3.3 m (Fig. 4).

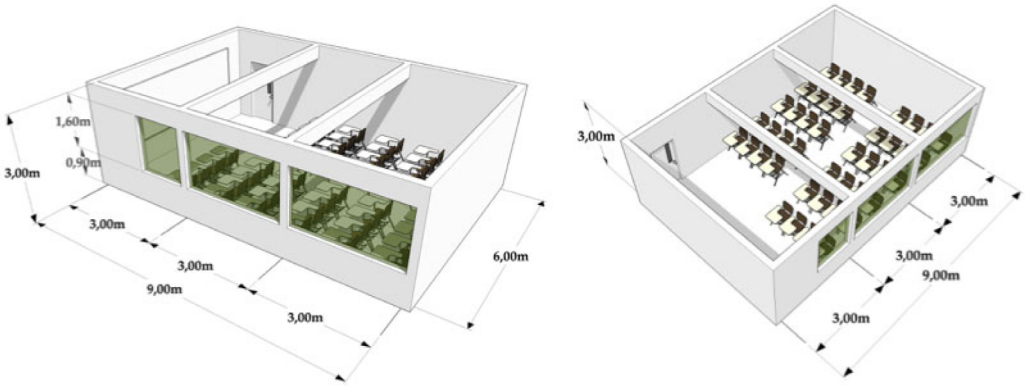

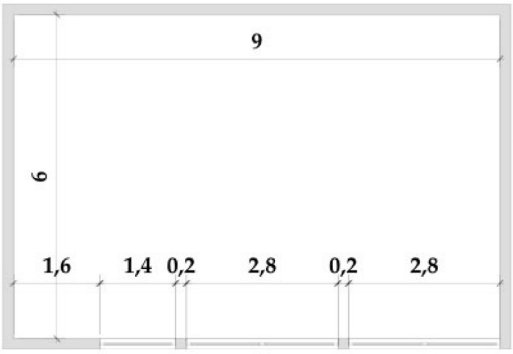

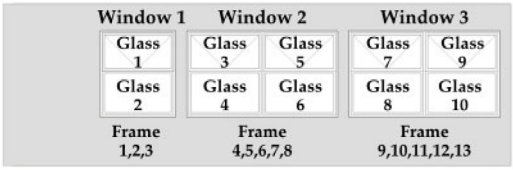

Name	Area	Height	Length	Frame total area
Frame 1	0,234	1,6	1,4	2,659
Frame 2	0,155	0,7	1,32	Glazing total area
Frame 3	0,165	0,82	1,32	8,541
Frame 4	0,406	1,6	2,8	Window total area
Frame 5	0,157	0,7	1,34	11,2
Frame 6	0,166	0,82	1,34	Opening area
Frame 7	0,157	0,7	1,34	4,842
Frame 8	0,166	0,82	1,34	Window 1 Area
Frame 9	0,166	0,82	1,34	2,24
Frame 10	0,157	0,7	1,34	Window 2 Area
Frame 11	0,406	1,6	2,8	4,48
Frame 12	0,166	0,82	1,34	Window 3 Area
Frame 13	0,157	0,7	1,34	4,48
Glass 1	0,769	0,62	1,24	Premises Area
Glass 2	0,918	0,74	1,24	54
Glass 3	0,781	0,62	1,26	Window percentage
Glass 4	0,932	0,74	1,26	20,741
Glass 5	0,781	0,62	1,26	Opening percentage
Glass 6	0,932	0,74	1,26	8,967
Glass 7	0,781	0,62	1,26	Frame percentage
Glass 8	0,932	0,74	1,26	23,743
Glass 9	0,781	0,62	1,26	
Glass 10	0,932	0,74	1,26	

Fig. 2. Construction of a base model with SketchUp. 2D construction of the base model with VectorWorks and determination of areas and percentages associated with the glazed surfaces and window components.

Table 1
Shading factor for façade obstacles (corbel or overhang), MSF and its components, and setbacks.
Source: Preparation by Authors based on the Spanish Technical Building Code (Dirección General de Arquitectura, 1998).

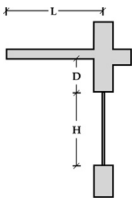

Orientation.		0.2 < L/H ≤ 0.5	0.5 < L/H ≤ 1	1 < L/H ≤ 2	L/H > 2
N	0 < D/H ≤ 0.2	0.82	0.5	0.28	0.16
	0.2 < D/H ≤ 0.5	0.87	0.64	0.39	0.22
	D/H > 0.5	0.93	0.82	0.6	0.39
NE/NW	0 < D/H ≤ 0.2	0.9	0.71	0.43	0.16
	0.2 < D/H ≤ 0.5	0.94	0.82	0.6	0.27
	D/H > 0.5	0.98	0.93	0.84	0.65
E/W	0 < D/H ≤ 0.2	0.92	0.77	0.55	0.22
	0.2 < D/H ≤ 0.5	0.96	0.86	0.7	0.43
	D/H > 0.5	0.99	0.96	0.89	0.75

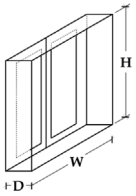

Orientation.		0.05 < D/W ≤ 0.1	0.1 < D/W ≤ 0.2	0.2 < D/W ≤ 0.5	D/W > 0.5
N	0.05 < R/H ≤ 0.1	0.82	0.74	0.62	0.39
	0.1 < R/H ≤ 0.2	0.76	0.67	0.56	0.35
	0.2 < R/H ≤ 0.5	0.56	0.51	0.39	0.27
	R/H > 0.5	0.35	0.32	0.27	0.17
NE/NW	0.05 < R/H ≤ 0.1	0.86	0.81	0.72	0.51
	0.1 < R/H ≤ 0.2	0.79	0.74	0.66	0.47
	0.2 < R/H ≤ 0.5	0.59	0.56	0.47	0.36
	R/H > 0.5	0.38	0.36	0.32	0.23
E/W	0.05 < R/H ≤ 0.1	0.91	0.87	0.81	0.65
	0.1 < R/H ≤ 0.2	0.86	0.82	0.76	0.61
	0.2 < R/H ≤ 0.5	0.71	0.68	0.61	0.51
	R/H > 0.5	0.53	0.51	0.48	0.39

Table 2
Boundary conditions of simulations: loads, setpoints, and values.

Loads	Units	Value	Schedule
Natural ventilation	Ac/h	5	Monday to Friday 8 am to 6 pm
Infiltration	Ac/h	0.7	Annual
General lighting-normalized power density	W/m^2-100 lux	2.5	Monday to Friday 8 am to 6 pm
Occupancy density	people/m^2	0.5	Monday to Friday 8 am to 6 pm
Cooling	°C	24	Monday to Friday 8 am to 6 pm
Heating	°C	21	Monday to Friday 8 am to 6 pm
Lighting control	Lux	400 work plane height 0.8 m	Monday to Friday 8 am to 6 pm

Table 3
Glazing used and its optical and thermal characteristics.
Source: Preparation by the authors based on DesignBuilder (*) and LBNL Window data.

Glazing	ID	Thickness mm	ST	SR1	SR2	VT	VR1	VR2	IRT	emis1	emis2	Con W/mK
0.82*	Generic	6.000	0.820	0.074	0.074	0.900	0.081	0.081	0	0.840	0.840	1.000
0.90	14 708	5.800	0.902	0.080	0.080	0.911	0.083	0.083	0	0.840	0.840	1.000
0.85	21 013	6.000	0.849	0.075	0.075	0.900	0.081	0.081	0	0.840	0.840	1.000
0.72	3293	5.613	0.725	0.092	0.092	0.866	0.091	0.092	0	0.840	0.840	1.000
0.70	21 547	6.360	0.703	0.074	0.072	0.840	0.082	0.081	0	0.840	0.840	0.818
0.51	5067	5.660	0.512	0.055	0.055	0.629	0.062	0.062	0	0.840	0.840	1.000
0.41	9834	5.918	0.408	0.050	0.050	0.438	0.052	0.052	0	0.840	0.840	1.000
0.27	17 000	5.740	0.267	0.180	0.094	0.418	0.194	0.172	0	0.839	0.840	1.000
0.19	16 122	6.107	0.189	0.254	0.256	0.240	0.279	0.266	0	0.840	0.840	0.812
0.16	17 019	5.880	0.160	0.303	0.080	0.193	0.329	0.116	0	0.842	0.840	1.000
0.15	9611	5.691	0.147	0.254	0.299	0.172	0.231	0.226	0	0.840	0.773	0.985

ID: From the LBNL Window database, except for 0.82*; ST: Solar Transmission Factor; SR: Solar Reflectance Factor; VT: Visible transmission factor; VR: Visible reflectance factor; IRT: infrared transmission factor; emis: emissivity; Con: thermal conductivity.

Table 4
MSF values by orientation for overhang depths between 0.1 and 4.0 m, considering an aluminum profile with half white TBB (Thermal Bridge Break) and single glazing.

Overhang length (m)	Modified solar factor		
	N	NE–NW	E–W
0.10–0.80	0.54	0.59	0.60
0.90–1.60	0.33	0.47	0.51
1.70–3.20	0.18	0.28	0.36
3.30–4.00	0.11	0.11	0.14

The MSF value varied significantly in the North orientation, differentiating most between 0.8 and 0.9 m; in the NE–NW orientation between 1.6–1.7 m; and in the E–W orientation, between 3.2–3.3 m. Above 3.3 m, values associated with MSF tend to be coupled, with their value being close to 0.1.

To compare the values obtained when using glazing and an overhang, the following relationship table is established (Table 5), where MSF values obtained by numerical calculation for the different overhang length ranges, can be compared with the ST value of the glazing, to evaluate similar energy consumption.

3.2. Heating and cooling results

The results show that for Talca, energy is required for cooling, and to a lesser extent, for heating, which occurs only in some orientations for the case study. The period with the highest cooling energy consumption takes place between November and April, and its lowest point is seen between June and July, which repeats for all orientations, with the most marked differences being with the North orientation. The South orientation, despite not being considered within the heat-carrying orientations, has similar behavior, although with much more reduced requirements.

The cooling graphs show differences between the results obtained with setbacks and with overhangs. For the North orientation, the maximum energy consumption value for setbacks is greater than that for overhangs. The curve associated with the lowest protection level, ST 0.5–0.3, and overhangs of dimensions close to 1.5 or higher, tend to generate similar curves, but the curve of overhang protections falls constantly from January to April, maintaining values close to zero during April and October, unlike setbacks which tend to move to the minimum value between May and August.

The curves are similar for the East and West orientations. However, lower energy consumption values are seen on the curves generated by overhangs of 2.5 m or longer. An energy consumption close to zero is seen over a longer period for overhang solutions, reaching October, compared to September in the case of setbacks.

For Northeast and Northwest orientations, the curves have similar behaviors for setbacks and overhangs, but with higher peaks for overhangs, and also longer consumption periods close to zero. For the case of setbacks, the close-to-zero period is between May and September, while for overhangs, it is between May and October.

For the South orientation, the curves are similar, with setback protections having less consumption than all the curves generated by the overhang protection.

The heating requirements mostly occur between April and October, with their peak in July. This requirement is seen on the East, West, and South orientations for setback protections, and overhangs on the North, East, West, and South orientations, with overhangs having a lower energy consumption (Fig. 6).

The cooling energy consumption graphs are presented comparatively in Figs. 3, 4, and 5, and those of heating energy consumption in Fig. 6. The top row shows the results for setback protection, and the bottom row, for protection by an overhang.

To build the graphs, the values obtained for cooling energy consumption are used as a reference, given that they have the highest values and variation. The cooling energy consumption values associated with overhangs with the same MSF value are associated with the energy consumption values obtained with setbacks and their equivalent values.

This allows obtaining a curve where it is seen that, for all cases, the use of solar protection through the overhang is more efficient over the annual period for cooling-associated energy consumption than the use of solar control glass. The tables show, for each orientation, a curve associated with the energy consumption value of each overhang value on the *y*-axis, and for the glass g

Table 5
MSF values for overhang lengths between 0.1 and 4.0 m, and their relationship by orientation with the ST values of the glazing used in the case study.

	Orientation	MSF	ST Glazing-overhang	ST Glazing-setback
Overhang 0.1–0.8 (m) – setback 0.1 (m)	N	0.54	0.82	0.85
	NE–NW	0.59	0.82	0.90
	E–W	0.6	0.82	0.85
Overhang 0.9–1.6 (m) – setback 0.1 (m)	N	0.33	0.82	0.51
	NE–NW	0.47	0.82	0.70
	E–W	0.51	0.82	0.72
Overhang 0.7–3.2 (m) – setback 0.1 (m)	N	0.18	0.82	0.27
	NE–NW	0.28	0.82	0.41
	E–W	0.36	0.82	0.51
Overhang 3.3–4.0 (m) – setback 0.1 (m)	N	0.11	0.82	0.16
	NE–NW	0.11	0.82	0.15
	E–W	0.14	0.82	0.19

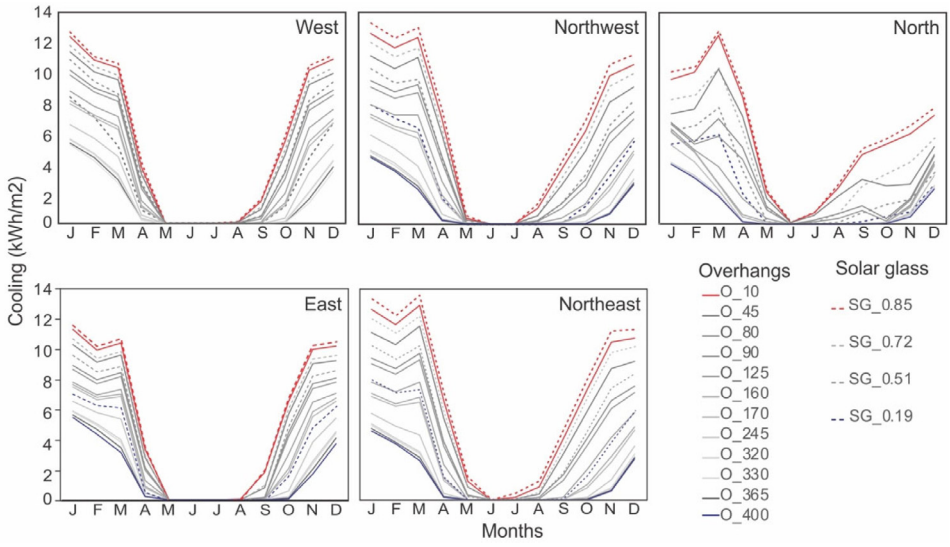

Fig. 3. Monthly energy consumption for cooling by orientation for overhangs (Length of 10 mm to 400 mm) and solar control glass.

value equivalent to the MSF of the overhang on the *x*-axis. Cooling energy consumption comparison graphs are shown in Fig. 4.

The graphs in Fig. 5 show that, for the case of cooling energy consumption through overhang protection, for the North orientation, the values that have the greatest differences are for an 80 cm deep overhang versus ST 0.85, equivalent to MSF 0.54 with an energy consumption of 34.06 kWh × m^2 year (overhang), versus 72.72 kWh × m^2 year (setback), and the minimums for a 10 cm deep overhang versus ST 0.85, equivalent to MSF 0.54, with an energy consumption of 68.90 kWh × m^2 year (overhang), versus 72.72 kWh × m^2 year (setback). Both extreme differences occur for the same MSF segment. For the Northeast orientation, the maximums are a 320 cm overhang versus ST 0.41, equivalent to MSF 0.28, with an energy consumption of 16.54 kWh × m^2 year (overhang), versus 56.23 kWh × m^2 year (setback), and the minimums for a 10 cm deep overhang versus ST 0.9, with an energy consumption of 78.70 kWh × m^2 year (overhang), versus 84.86 kWh × m^2 year (setback). For the Northeast orientation, the maximums are 160 cm overhang versus ST 0.70, equivalent to MSF 0.47, with an energy consumption of 29.86 kWh × m^2 year (overhang), versus 69.76 kWh × m^2 year (setback), and the minimums for a 10 cm deep overhang versus ST 0.9, with an energy consumption of 75.14 kWh × m^2 year (overhang), versus 81.13 kWh × m^2 year (setback). For the East orientation, the maximums are 320 cm overhang versus ST 0.51, equivalent to MSF 0.36, with an energy consumption of 22.61 kWh × m^2 year (overhang), versus 51.18 kWh × m^2 year (setback), and the minimums for a 10 cm deep overhang versus ST 0.85, with an energy consumption of 63.71 kWh × m^2 year (overhang), versus 65.68 kWh × m^2 year (setback). For the West orientation, the maximums are 320 cm overhang versus ST 0.51, equivalent to MSF 0.36, with an energy consumption of 20.29 kWh × m^2 year (overhang), versus 52.87 kWh × m^2 year (setback), and the minimums for 10 cm deep overhang versus ST 0.85, with an energy consumption of 65.36 kWh × m^2 year (overhang), versus 67.39 kWh × m^2 year (setback).

3.3. Lighting results

For lighting needs, it is seen that the demand increases in April, and reaches its peak between May and July, falling in August until reaching troughs between December and February.

It can be seen that in the North orientation, the curves associated with values of 0.3 to 0.6 tend to couple, generating a marked separation between 0.2 and 0.1. For the case of overhangs, the curves separate into two groups: those less than 1.6 m, and those equal to or greater than 1.6 m in depth.

For the East orientation, the curves have similar behavior, but with a greater energy requirement at its peak. However, the troughs are below those seen in the North orientation. The same uncoupling of the curves occurs in overhangs, concentrating on those of less than 1.6 m in depth, separated from the others.

For the West orientation, the solar control glass protection shows similar curves in all cases, evidencing a separation between the values of 0.1 and 0.2 with respect to the other curves. For the case of overhang protection, the curves show similar

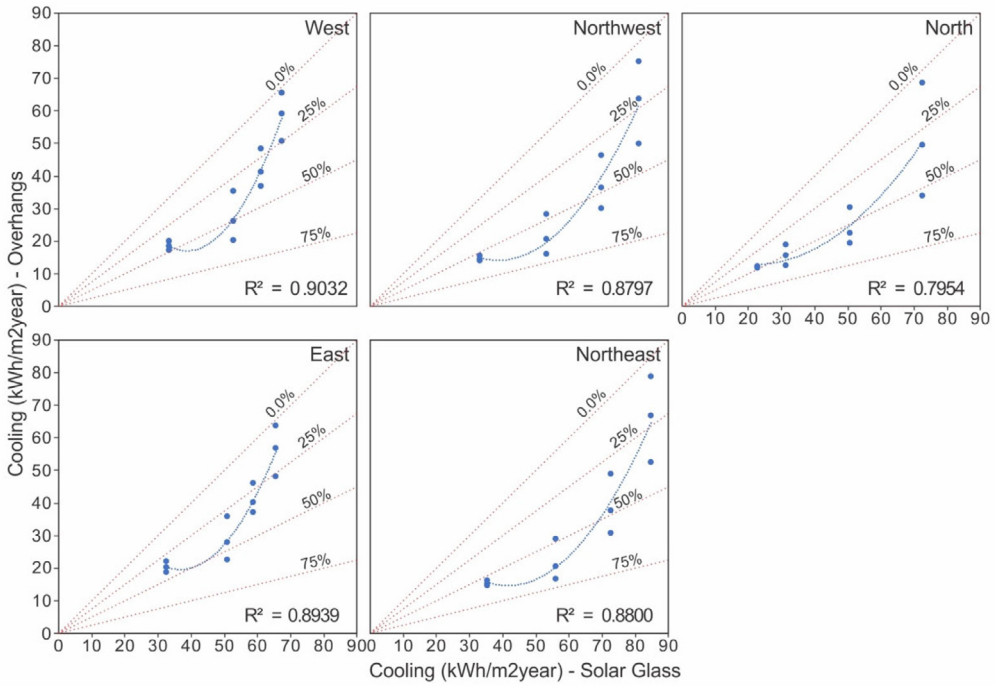

Fig. 4. Comparison of cooling energy consumption of overhang v/s setback with solar control glass, for the different orientations.

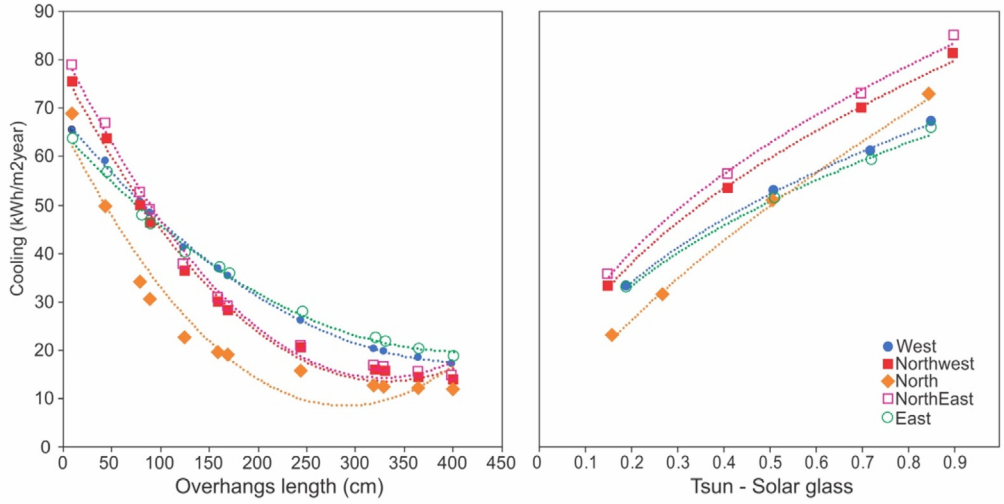

Fig. 5. Comparison of cooling energy consumption by overhang length (top row) and cooling energy consumption for the setback with solar control glass (bottom row). Both cases for the different orientations.

behavior to the East orientation, with two separate groups of curves.

For the Northeast orientation, the solar control glass and overhang curves are similar at their peaks and troughs, with the 0.1 glass curve having a different behavior. The energy consumption curves for overhangs are below those for setbacks.

For the Northeast orientation, overhang curves tend to be lower compared to those for setbacks, maintaining the uncoupling of the two groups of curves.

For the South orientation, energy requirements are lower in the case of overhangs, with curves that are similar to the glass, with troughs within similar periods, but peaks at lower values.

The lighting energy consumption graphs are presented comparatively in Fig. 7. The top row shows the results for the protection by the setback, and the bottom row, for overhang protection.

For the case of energy consumption associated with lighting, it is seen that the use of solar control glass tends to be more efficient in some cases, associated with lower solar protection levels. However, when the MSF value is higher, the use of overhangs is more efficient on North, Northeast, and Northwest orientations. For East and West orientations, the efficiency of solar control glass is more noticeable. Graphs comparing lighting energy consumption are shown in Fig. 8.

3.4. Comparison of total consumption

Table 6 shows the annual consumption values associated with each orientation for each overhang depth and the setback associated with the same MSF. The values that appear in the colored cells indicate that the energy consumption associated with the setback is greater than that for the overhang. It is seen

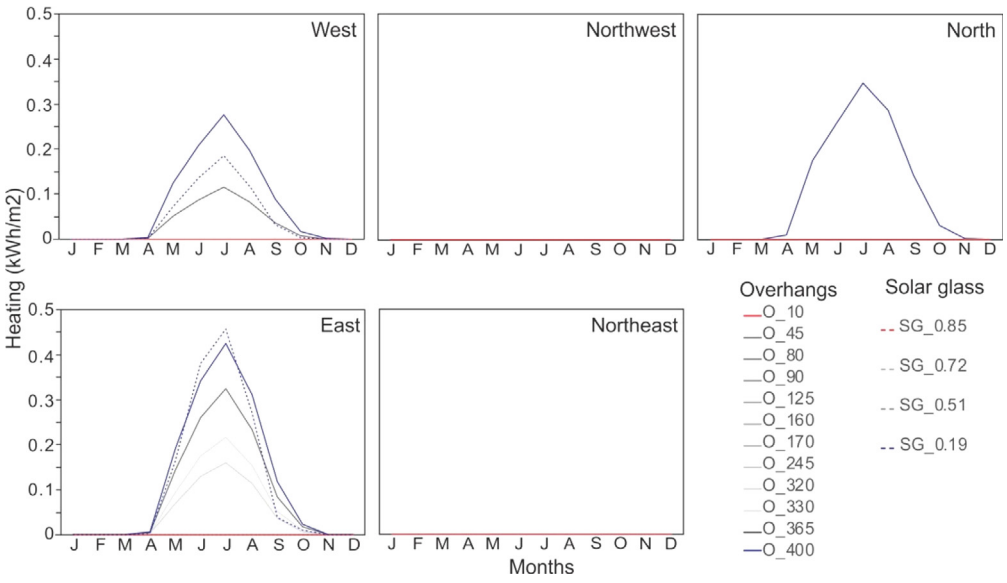

Fig. 6. Monthly heating energy consumption by orientation with overhang (length of 10 mm to 400 mm) and solar control glass.

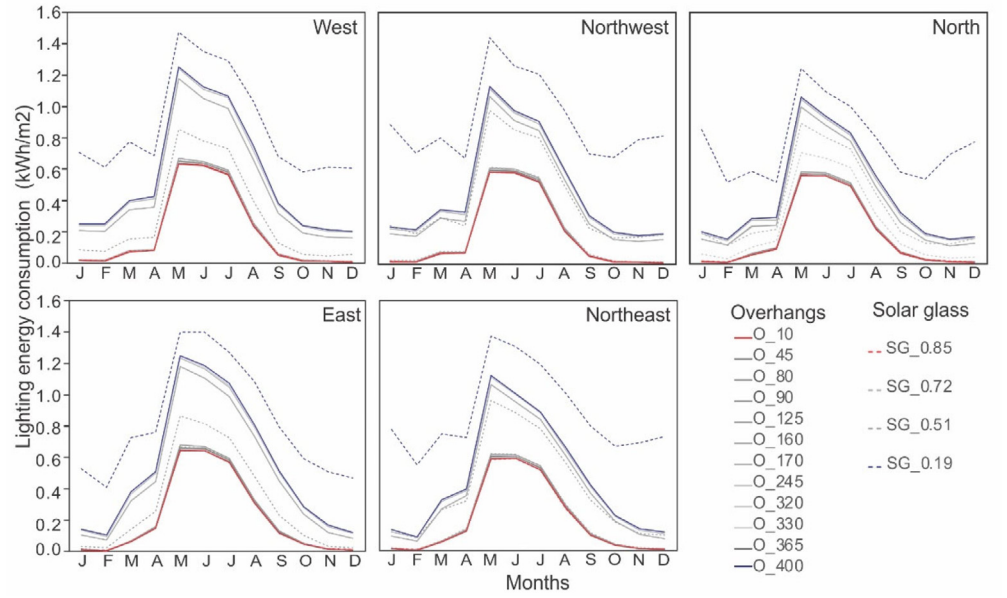

Fig. 7. Lighting energy consumption by orientation for overhangs (length of 10 mm to 400 mm) and solar control glass.

that from the 48 values associated by orientation, for the North, East, and West orientations, 30/48 (62.5%) are obtained, being more efficient for overhangs, and for Northeast and Northwest orientations, 29/48 (60.4%).

From the 60 values obtained for overhangs in the 5 orientations evaluated, 4 cases, equivalent to 6.67%, were more efficient for heating energy consumption; 100% were more efficient in cooling energy consumption; 40% (24 cases) were more efficient in lighting energy consumption, and 100% were more efficient in the values associated to total energy consumption.

The analysis of the results using RStudio software provided results for the regression model indicated in Table 7, for all the studied orientations.

For the R2 value, corresponding to the model's effectiveness, a value of 0.7783, equivalent to 78%, was obtained, which indicates that both variables together, overhang and glass, explain the Total Energy Consumption result. The adjusted R2 value was slightly lower at 0.7725. The p-value (contrast statistic) is less than 0.05, which is why it is considered valid with a significance of the variables that exceeds 99.9%.

3.5. Discussion

The location required 60 thermal energy and lighting simulations associated with overhang lengths in the five defined orientations (N, NE, NW, E, and W), plus 20 simulations for setback values, using the same orientations. This is done under a "shoebox"-type model, although with characteristics closer to a classroom typology, bearing in mind that these preliminary models allow initial approaches, and do not always represent reality (Ayoub, 2019). These results generated possible comparison curves to determine the similarities or differences in energy consumption using solar protection or overhangs, considering single glazing and an aluminum frame with clear white TBB.

It could be seen that the MSF calculation associated with overhang length varies depending on the orientation, causing sections

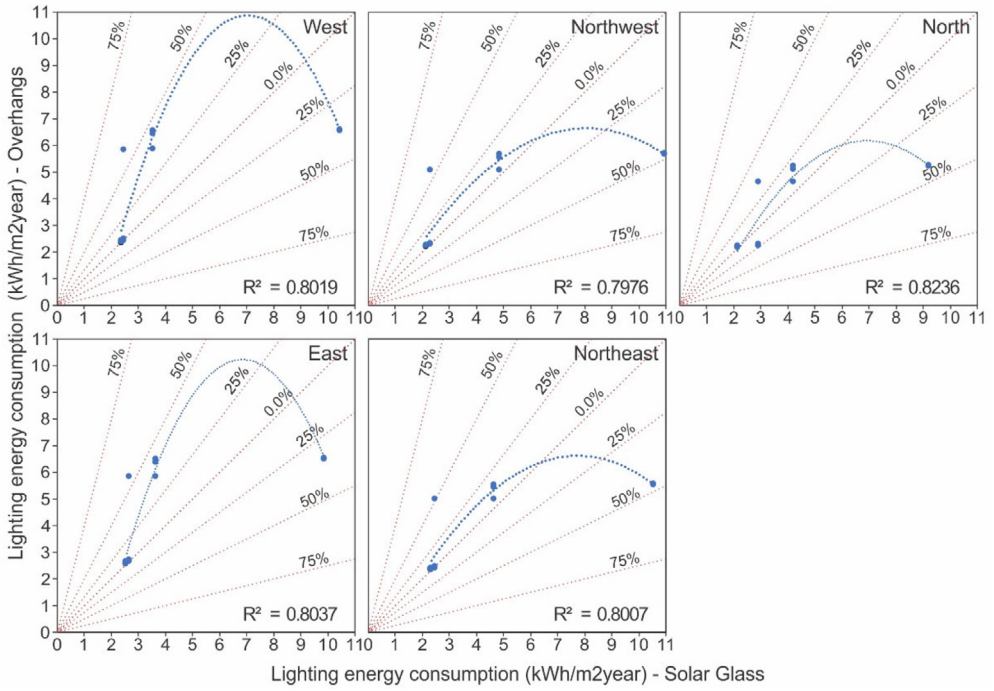

Fig. 8. Comparison of lighting energy consumption of overhang v/s setback with solar control glass, for the different orientations.

Table 6
Differences in heating, cooling, lighting, and total energy consumption, by orientation for each setback versus overhang value, and their associated MSF value, in kWh year.

Differences in annual energy consumption – setback vs. overhang – North orientation (kWh year)												
Consumption energy	MSF 0.54	MSF 0.54	MSF 0.54	MSF 0.33	MSF 0.33	MSF 0.33	MSF 0.18	MSF 0.18	MSF 0.18	MSF 0.11	MSF 0.11	MSF 0.11
Heating	0.00	0.00	0.00	0.00	0.00	0.00	0.00	0.00	0.00	0.00	−1.25	−1.25
Cooling	3.82	23.01	38.66	20.20	28.21	31.19	12.29	15.54	18.76	10.46	10.84	11.06
Lighting	0.00	−0.01	−0.06	0.70	0.65	−1.69	−0.39	−0.84	−0.98	4.04	4.03	4.02
Total	3.82	22.99	38.59	20.90	28.85	29.50	11.90	14.70	17.78	14.49	13.62	13.83
Differences in annual energy consumption – setback vs. overhang – East orientation (kWh year)												
	MSF 0.60	MSF 0.60	MSF 0.60	MSF 0.51	MSF 0.51	MSF 0.51	MSF 0.36	MSF 0.36	MSF 0.36	MSF 0.14	MSF 0.14	MSF 0.14
Heating	0.00	0.00	0.00	0.00	0.00	0.00	0.00	0.00	−0.52	0.62	0.25	−0.09
Cooling	1.97	8.98	17.73	12.96	18.98	21.91	15.41	23.21	28.57	10.77	12.41	13.97
Lighting	0.00	−0.02	−0.08	0.01	−0.06	−3.17	−2.16	−2.68	−2.80	3.40	3.40	3.37
Total	1.97	8.96	17.65	12.97	18.92	18.74	13.25	20.53	25.25	14.79	16.06	17.24
Differences in annual energy consumption – setback vs. overhang – West orientation (kWh year)												
	MSF 0.60	MSF 0.60	MSF 0.60	MSF 0.51	MSF 0.51	MSF 0.51	MSF 0.36	MSF 0.36	MSF 0.36	MSF 0.14	MSF 0.14	MSF 0.14
Heating	0.00	0.00	0.00	0.00	0.00	0.00	0.00	0.00	0.00	0.55	0.17	−0.36
Cooling	2.03	8.41	16.74	12.95	20.04	24.42	17.52	26.68	32.58	13.54	15.04	16.15
Lighting	0.00	−0.02	−0.08	0.00	−0.06	−3.40	−2.34	−2.92	−3.05	3.87	3.87	3.84
Total	2.03	8.39	16.66	12.95	19.98	21.01	15.18	23.75	29.54	17.96	19.08	19.63
Differences in annual energy consumption – setback vs. overhang – Northeast orientation (kWh year)												
	MSF 0.59	MSF 0.59	MSF 0.59	MSF 0.47	MSF 0.47	MSF 0.47	MSF 0.28	MSF 0.28	MSF 0.28	MSF 0.11	MSF 0.11	MSF 0.11
Heating	0.00	0.00	0.00	0.00	0.00	0.00	0.00	0.00	0.00	0.00	0.00	0.00
Cooling	6.16	18.16	32.57	24.13	35.40	42.28	27.33	35.70	39.69	19.17	20.19	20.90
Lighting	−0.02	−0.04	−0.09	0.06	0.01	−2.52	−0.34	−0.77	−0.88	5.01	5.01	5.00
Total	6.14	18.13	32.48	24.20	35.41	39.77	27.00	34.93	38.81	24.18	25.20	25.90
Differences in annual energy consumption – setback vs. overhang – Northwest orientation (kWh year)												
	MSF 0.59	MSF 0.59	MSF 0.59	MSF 0.47	MSF 0.47	MSF 0.47	MSF 0.28	MSF 0.28	MSF 0.28	MSF 0.11	MSF 0.11	MSF 0.11
Heating	0.00	0.00	0.00	0.00	0.00	0.00	0.00	0.00	0.00	0.00	0.00	0.00
Cooling	5.99	17.58	31.41	23.65	33.58	39.90	25.19	33.00	37.48	17.82	18.97	19.54
Lighting	−0.02	−0.04	−0.09	0.06	0.00	−2.74	−0.20	−0.67	−0.79	5.30	5.29	5.28
Total	5.97	17.54	31.32	23.71	33.58	37.16	24.99	32.33	36.69	23.11	24.26	24.82

Note: A value above zero indicates that energy consumption associated with a setback is higher than that associated with an overhang.

Table 7
Values for the regression model considering Total Energy, Overhangs, and Glass.

Parameter	Estimation	Standard error	t value	p-value	Significance
Intercept	38.5523	4.2553	9.066	8.94e−14	0.001
Overhang	−13.1536	0.8021	−16.399	<2e−16	0.001
ST_ Glass	32.6187	5.9611	5.472	5.35e−07	0.001

with constant values at certain lengths, and significant variations on passing from one value to another in certain periods. These sections vary depending on the geometry of the opening.

These significant variations are not seen in the analysis of heating–cooling energy consumption, but are in the analysis of monthly lighting, where coupled curves appeared up to a certain size, which is separated in other sections, with a clear differentiation regarding energy consumption.

These differences occur when the overhang reaches 1.6 m in depth, while lengths of 1.6 m or less provide smaller and similar values.

For values of 1.6 or less, the MSF calculation results in 0.33 to 0.60. However, the difference between applying an overhang of under 1.6 m and one of 1.6 m of depth or greater, can double energy demand for lighting, although this is significantly lower than that for cooling.

Likewise, applying glazing of ST 0.57 or ST 0.49 for overhang sections of 0.1 to 0.80 m, and 0.90 to 1.60 m, generates, in this case study, a difference in cooling demand of approximately between 15 and 35 kWh/m^2 year, depending on the orientation this is applied to.

It could be seen that there are significant variations in total energy consumption between the application of solar protection through glazing and the use of overhangs. This spread of results within the same MSF value can be seen in Fig. 9, for each one of these values. This indicates an energy response that can be differentiated depending on the strategy and location where it is used. A location defined by the climate file chosen for this purpose can also contribute with variations that may or may not be relevant for the energy consumption results (Bellia et al., 2015). Opting for any of these alternatives during early decision-making would help to define solar protection levels to calibrate energy contributions, benefiting energy savings. Meanwhile, achieving optimal energy performance requires evaluating the relationship and dependence between both requirements, conditioned by the solar protection in one location considering the orientation and use of the building.

On observing thermal and light behavior curves, it can be assumed that the assessment of solar protections requires simultaneous analysis of thermal and lighting parameters, from a numerical calculation to the definition of a seasonal variation of the requirement to find a suitable and effective combination. Likewise, it is possible to determine a similar total energy behavior between glass and overhang, but not necessarily within an equivalent MSF section, given that the variation of the lighting energy consumption may affect the total value. This also needs to be assessed on a case-by-case basis, as the geometry of the opening (Hiyama and Wen, 2015) and its optical characteristics have an important effect on the determination of the MSF, being able to move the MSF equivalent between overhangs and glass.

These considerations are relevant, on being part of Standards whose application can be ineffective, or lead to different conditions than those foreseen (Tregenza and Mardaljevic, 2018), especially when these are considered in early decision-making stages, that seek a sustainable design and, because of this, less environmental damage (Bakmohammadi and Noorzai, 2020).

The following points are considered as limitations for this study

1. The use of just one combination of characteristics associated with the opening, both in its geometry and optical properties, which have an important impact on the MSF calculation.
2. The premises assessed is a school classroom, defining a limiting occupation time.
3. The analysis was made in an annual period, from January to December, without discounting the summer and winter vacation periods, which are critical periods for energy demand, both in heating/cooling and in daylight, which would partially reflect the condition of a classroom in this location.
4. Interior finishings have not been considered on the walls, with only outside insulation and reinforced concrete for all construction elements able to have an impact on the thermal losses and inertia of the premises.
5. A building was considered with just one exposed façade, leaving out situations in contact with the ground, higher floors, or corner rooms with two or more exposed faces.
6. It was applied in one location in Chile, so it is not possible to extrapolate the results to other similar conditions.
7. The climate file was taken from the Meteonorm v. 7.0 software, being able, in some cases, to extrapolate values of locations that do not have exactly the same local climate variations.
8. The glass used for the base case has been defined as generic, using the DesignBuilder database, which is why it does not represent real glass in all of its dimensions. The rest of the glazing is from the database of the LBNL Window software and is associated with a real product.
9. The glazed surfaces have been defined as single glazing without a watertight double glazing solution, as suggested by the new recommendations for school premises.
10. The statistical analysis only considered the properties of glass and the length of the overhang on the total energy consumption, leaving aside other variables of the opening that can have an important effect on energy savings, along with the orientation of the glazed surface (Susorova et al., 2013).

The analysis of the results opens up the discussion on the recommendations of solar control strategies, which do not simultaneously consider the impact these have on daylight contributions. The interest in solving overheating problems can have a negative impact on the strategy being used if an uncritical use of glass or overhangs is considered, even when both strategies can provide the same result through the MSF calculation. Similarly, it is clear that certain orientations and strategies may be more critical than others, generating conflict between both target requirements (Futrell et al., 2015).

The research requires detailing, in different scenarios, whether varying the window-to-wall ratio is considered or is applied to other activities, added to the evaluation of those strategies that are more common in each local reality, given that the geometry and materials in the opening group have a great impact on lighting and thermal behavior. Considering those more commonly applied may be beneficial and necessary in early decision-making (Pilechiha et al., 2020).

4. Conclusions

The findings allow seeing that the implementation of solar protection using setbacks and solar glass versus implementing an overhang-based solution, using equal solar protection values, be it through MSF or with the ST value of the glass, can produce different lighting and thermal results. These variations become clearer

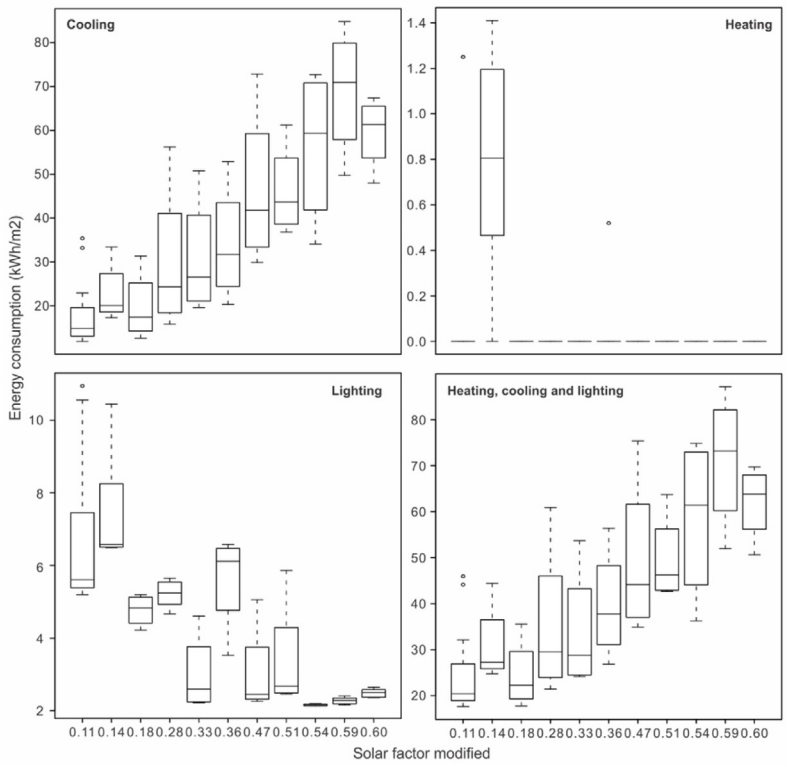

Fig. 9. Energy consumption graphs of cooling, heating, lighting, and total energy versus the MSF.

when found in certain ranges of overhang depth that affect lighting behavior, demonstrating a progressive growth behavior in thermal performances, but differentiated by orientation.

These results suggest evaluating solar protection strategies early to recommend the most pertinent ones, considering the results of the MSF calculation and, simultaneously, those of energy simulation, integrating the benefits and disadvantages that each solar protection system offers in one year, both in thermal and in lighting aspects. Despite this, this experiment has been applied considering one case and the variables have been limited, simulating within specific climate conditions, as such it needs to be extended to other locations, opening geometries, arrangements of the opening set, and construction combinations to verify their variations and scopes.

CRediT authorship contribution statement

Cristián Muñoz-Viveros: Conceptualization, Data curation, Formal analysis, Research, Methodology, Project management, Resources, Software, Visualization, Writing. **Alexis Pérez-Fargallo:** Methodology, Project management, Supervision, Validation, Writing. **Carlos Rubio-Bellido:** Supervision, Writing – review & editing.

Declaration of competing interest

The authors declare that they have no known competing financial interests or personal relationships that could have appeared to influence the work reported in this paper.

Acknowledgments

The authors acknowledge the support provided by "Confort Ambiental *y* Pobreza Energética" research group of the Universidad del Bío-Bío, Chile (GI/C 19450) and the Thematic Network 722RT0135 "Red Iberoamericana de Pobreza Energética *y* Bienestar Ambiental" (RIPEBA) financed by the call for Thematic Networks of the CYTED Program for 2021. The authors would like to thank the guidance and support of Architect Laura Marín R., Ph.D., of the University of Bío-Bío, in the preparation of the first manuscript.

References

Acosta, I., Campano, Molina, J.F., 2016. Window design in architecture: Analysis of energy savings for lighting and visual comfort in residential spaces. Appl. Energy 168, 493–506. http://dx.doi.org/10.1016/j.apenergy.2016.02.005.

Ahmad, R.M., El-Sayed, Z., Taha, D., Shokry, H., Mahmoud, H., 2021. An approach to select an energy-efficient shading device for the south-oriented façades in heritage buildings in Alexandria, Egypt. Energy Rep. 7, 133–137. http://dx.doi.org/10.1016/j.egyr.2021.06.024.

Al-Khatatbeh, B.J., Ma'Bdeh, S.N., 2017. Improving visual comfort and energy efficiency in existing classrooms using passive daylighting techniques. Energy Procedia 136, 102–108. http://dx.doi.org/10.1016/j.egypro.2017.10.294.

Alhagla, K., Mansour, A., Elbassuoni, R., 2019. Optimizing windows for enhancing daylighting performance and energy saving. Alexandria Eng. J. 58, 283–290. http://dx.doi.org/10.1016/j.aej.2019.01.004.

Alwetaishi, M., Taki, A., 2020. Investigation into energy performance of a school building in a hot climate: Optimum of window-to-wall ratio. Indoor Built Environ. 29, 24–39. http://dx.doi.org/10.1177/1420326X19842313.

Ashrafian, T., Moazzen, N., 2019. The impact of glazing ratio and window configuration on occupants' comfort and energy demand: The case study of a school building in Eskisehir, Turkey. Sustain. Cities Soc. 47, 101483. http://dx.doi.org/10.1016/j.scs.2019.101483.

Ayoub, M., 2019. 100 Years of daylighting: A chronological review of daylight prediction and calculation methods. Sol. Energy 194, 360–390. http://dx.doi.org/10.1016/J.Solener.2019.10.072.

Bakmohammadi, P., Noorzai, E., 2020. Optimization of the design of the primary school classrooms in terms of energy and daylight performance considering occupants' thermal and visual comfort. Energy Rep. 6, 1590–1607. http://dx.doi.org/10.1016/j.egyr.2020.06.008.

Bellia, L., Pedace, A., Fragliasso, F., 2015. Dynamic daylight simulations: Impact of weather file's choice. Sol. Energy 117, 224–235. http://dx.doi.org/10.1016/j.solener.2015.05.002.

Boafo, F.E., Ahn, J.G., Kim, S.M., Kim, J.H., Kim, J.T., 2019. Fenestration refurbishment of an educational building: Experimental and numerical evaluation of daylight, thermal and building energy performance. J. Build. Eng. 25, 100803. http://dx.doi.org/10.1016/j.jobe.2019.100803.

Bodart, M., De Herde, A., 2002. Global energy savings in offices buildings by the use of daylighting. Energy Build. 34, 421–429. http://dx.doi.org/10.1016/S0378-7788(01)00117-7.

Bustamante, W., Encinas, F., Otárola, R., Pino, A., 2012. Análisis de estrategias para confort térmico y lumínico de edificios en diferentes climas de la Zona Central de Chile. ARQ (82), 112–115.

Carlos, J.S., 2017. The impact of refurbished windows on Portuguese old school buildings. Archit. Eng. Des. Manage. 13, 185–201. http://dx.doi.org/10.1080/17452007.2016.1274252.

Carlucci, S., Causone, F., Rosa, F.De., Pagliano, L., 2015. A review of indices for assessing visual comfort with a view to their use in optimization processes to support building integrated design. Renew. Sustain. Energy Rev. 47, 1016–1033. http://dx.doi.org/10.1016/j.rser.2015.03.062.

Cheong, K.H., Teo, Y.H., Koh, J.M., Acharya, U.R., Man Yu, S.C., 2020. A simulation-aided approach in improving thermal-visual comfort and power efficiency in buildings. J. Build. Eng. 27, 100936. http://dx.doi.org/10.1016/j.jobe.2019.100936.

Chi, D.A., Moreno, D., Navarro, J., 2018. Correlating daylight availability metric with lighting, heating and cooling energy consumptions. Build. Environ. 132, 170–180. http://dx.doi.org/10.1016/j.buildenv.2018.01.048.

CITEC-UBB, DECON-UC, Dirección de Arquitectura, M. de O.P., 2015. Términos de Referencia EstandArizados Con ParáMetros de Eficiencia Energética Y Confort Ambiental, Para Licitaciones de Diseño Y Obras de la Dirección de Arquitectura, Según Zonas GeográFicas Del País Y Según Tipología de Edificios _ Versión 2. Según Zo. Geográficas del País y Según Tipologías Edif.

Correia da Silva, P., Leal, V., Andersen, M., 2013. Occupants interaction with electric lighting and shading systems in real single-occupied offices: Results from a monitoring campaign. Build. Environ. 64, 152–168. http://dx.doi.org/10.1016/J.Buildenv.2013.03.015.

de Almeida Rocha, A.P., Reynoso-Meza, G., Oliveira, R.C.L.F., Mendes, N., 2020. A pixel counting based method for designing shading devices in buildings considering energy efficiency, daylight use and fading protection. Appl. Energy 262, 114497. http://dx.doi.org/10.1016/j.apenergy.2020.114497.

Dirección General de Arquitectura, V. y S.M. de F., 1998. DB_HE_abril_2009_50_53. Código Técnico la Edif.

Fang, Y., Cho, S., 2019. Design optimization of building geometry and fenestration for daylighting and energy performance. Sol. Energy 191, 7–18. http://dx.doi.org/10.1016/j.solener.2019.08.039.

Futrell, B.J., Ozelkan, E.C., Brentrup, D., 2015. Bi-objective optimization of building enclosure design for thermal and lighting performance. Build. Environ. 92, 591–602. http://dx.doi.org/10.1016/j.buildenv.2015.03.039.

Gasparella, A., Pernigotto, G., Cappelletti, F., Romagnoni, P., Baggio, P., 2011. Analysis and modelling of window and glazing systems energy performance for a well insulated residential building. Energy Build. 43, 1030–1037. http://dx.doi.org/10.1016/j.enbuild.2010.12.032.

Goia, F., Haase, M., Perino, M., 2013. Optimizing the configuration of a façade module for office buildings by means of integrated thermal and lighting simulations in a total energy perspective. Appl. Energy 108, 515–527. http://dx.doi.org/10.1016/j.apenergy.2013.02.063.

Hiyama, K., Wen, L., 2015. Rapid response surface creation method to optimize window geometry using dynamic daylighting simulation and energy simulation. Energy Build. 107, 417–423. http://dx.doi.org/10.1016/j.enbuild.2015.08.035.

Huang, Y., Niu, J., lei, Chung, ming, T., 2014. Comprehensive analysis on thermal and daylighting performance of glazing and shading designs on office building envelope in cooling-dominant climates. Appl. Energy 134, 215–228. http://dx.doi.org/10.1016/J.Apenergy.2014.07.100.

INE, 1997. Nch134/1.Of97 Vidrios planos - Ensayos - Parte 1, : Determinación de la transmisión de la luz, transmisión directa solar, transmisión de la energía solar total y transmisión ultravioleta, y factores de acristalamiento relacionados.

Jalali, Z., Noorzai, E., Heidari, S., 2020. Design and optimization of form and facade of an office building using the genetic algorithm. Sci. Technol. Built Environ. 26, 128–140. http://dx.doi.org/10.1080/23744731.2019.1624095.

Kirimtat, A., Krejcar, O., Ekici, B., Fatih Tasgetiren, M., 2019. Multi-objective energy and daylight optimization of amorphous shading devices in buildings. Sol. Energy 185, 100–111. http://dx.doi.org/10.1016/J.Solener.2019.04.048.

Kwon, C.W., Lee, K.J., 2018. Integrated daylighting design by combining passive method with daysim in a classroom. Energies 11, 1–17. http://dx.doi.org/10.3390/En11113168.

Larrumbide, E., Bedoya, C., 2015. El comportamiento del hueco de ventana en la arquitectura vernácula mediterránea española ante las necesidades de acondicionamiento solar. Inf. Constr. 67, e105. http://dx.doi.org/10.3989/ic.14.056.

Lartigue, B., Lasternas, B., Loftness, V., 2014. Multi-objective optimization of building envelope for energy consumption and daylight. Indoor Built Environ. 23, 70–80. http://dx.doi.org/10.1177/1420326X13480224.

Lee, J.W., Jung, H.J., Park, J.Y., Lee, J.B., Yoon, Y., 2013. Optimization of building window system in Asian regions by analyzing solar heat gain and daylighting elements. Renew. Energy 50, 522–531. http://dx.doi.org/10.1016/J.Renene.2012.07.029.

MINVU, 2017. Resumen de Modificaciones Y Rectificaciones de la Ordenanza General de Urbanismo Y Construcciones * Vigencia Desde Fecha Publicación Diario Oficial. D.S. FECHA VIGENCIA MATERIA.

Ochoa, C.E., Aries, M.B.C., van Loenen, E.J., Hensen, J.L.M., 2012. Considerations on design optimization criteria for windows providing low energy consumption and high visual comfort. Appl. Energy 95, 238–245. http://dx.doi.org/10.1016/j.apenergy.2012.02.042.

Ochoa, C.E., Capeluto, I.G., 2009. Advice tool for early design stages of intelligent facades based on energy and visual comfort approach. Energy Build. 41, 480–488. http://dx.doi.org/10.1016/j.enbuild.2008.11.015.

Østergård, T., Jensen, R.L., Maagaard, S.E., 2016. Building simulations supporting decision making in early design - A review. Renew. Sustain. Energy Rev. 61, 187–201. http://dx.doi.org/10.1016/j.rser.2016.03.045.

Pellegrino, A., Cammarano, S., Savio, V., 2015. Daylighting for green schools: A resource for indoor quality and energy efficiency in educational environments. Energy Proc. 78, 3162–3167. http://dx.doi.org/10.1016/J.Egypro.2015.11.774.

Pilechiha, P., Mahdavinejad, M., Pour Rahimian, F., Carnemolla, P., Seyedzadeh, S., 2020. Multi-objective optimisation framework for designing office windows: quality of view, daylight and energy efficiency. Appl. Energy 261, 114356. http://dx.doi.org/10.1016/j.apenergy.2019.114356.

Shaeri, J., Yaghoubi, M., Habibi, A., Chokhachian, A., 2019. The impact of archetype patterns in office buildings on the annual cooling, heating and lighting loads in hot-humid, hot-dry and cold climates of Iran. Sustain 11. http://dx.doi.org/10.3390/su11020311.

Shahbazi, Y., Heydari, M., Haghparast, F., 2019. An early-stage design optimization for office buildings' façade providing high-energy performance and daylight. Indoor Built Environ. 28, 1350–1367. http://dx.doi.org/10.1177/1420326X19840761.

Shan, R., 2014. Optimization for heating, cooling and lighting load in building façade design. Energy Procedia 57, 1716–1725. http://dx.doi.org/10.1016/j.egypro.2014.10.142.

Simmler, H., Binder, B., 2008. Experimental and numerical determination of the total solar energy transmittance of glazing with venetian blind shading. Build. Environ. 43, 197–204. http://dx.doi.org/10.1016/j.buildenv.2006.10.011.

Susorova, I., Tabibzadeh, M., Rahman, A., Clack, H.L., Elnimeiri, M., 2013. The effect of geometry factors on fenestration energy performance and energy savings in office buildings. Energy Build. 57, 6–13. http://dx.doi.org/10.1016/j.enbuild.2012.10.035.

Tregenza, P., Mardaljevic, J., 2018. Daylighting buildings: Standards and the needs of the designer. Light. Res. Technol. 50, 63–79. http://dx.doi.org/10.1177/1477153517740611.

Tsikra, P., Andreou, E., 2017. Investigation of the energy saving potential in existing school buildings in Greece, the role of shading and daylight strategies in visual comfort and energy saving. Proc. Environ. Sci. 38, 204–211. http://dx.doi.org/10.1016/j.proenv.2017.03.107.

Tzikopoulos, A.F., Karatza, M.C., Paravantis, J.A., 2005. Modeling energy efficiency of bioclimatic buildings. Energy Build. 37, 529–544. http://dx.doi.org/10.1016/j.enbuild.2004.09.002.

UNE-EN, 2011. UNE-EN 410 Determinación de las características luminosas y solares de los acristalamientos.

Uribe, D., Vera, S., Bustamante, W., McNeil, A., Flamant, G., 2019. Impact of different control strategies of perforated curved louvers on the visual comfort and energy consumption of office buildings in different climates. Sol. Energy 190, 495–510. http://dx.doi.org/10.1016/J.Solener.2019.07.027.

Vullo, P., Passera, A., Lollini, R., Prada, A., Gasparella, A., 2018. Implementation of a multi-criteria and performance-based procurement procedure for energy retrofitting of facades during early design. Sustain. Cities Soc. 36, 363–377. http://dx.doi.org/10.1016/j.scs.2017.09.029.

Wang, R., Lu, S., Feng, W., 2020. Impact of adjustment strategies on building design process in different climates oriented by multiple performance. Appl. Energy 266, 114822. http://dx.doi.org/10.1016/j.apenergy.2020.114822.

Xue, P., Li, Q., Xie, J., Zhao, M., Liu, J., 2019. Optimization of window-to-wall ratio with sunshades in China low latitude region considering daylighting and energy saving requirements. Appl. Energy 233–234, 62–70. http://dx.doi.org/10.1016/j.apenergy.2018.10.027.

Zhai, Y., Wang, Y., Huang, Y., Meng, X., 2019. A multi-objective optimization methodology for window design considering energy consumption, thermal environment and visual performance. Renew. Energy 134, 1190–1199. http://dx.doi.org/10.1016/j.renene.2018.09.024.

Zhang, A., Bokel, R., van den Dobbelsteen, A., Sun, Y., Huang, Q., Zhang, Q., 2017. Optimization of thermal and daylight performance of school buildings based on a multi-objective genetic algorithm in the cold climate of China. Energy Build. 139, 371–384. http://dx.doi.org/10.1016/j.enbuild.2017.01.048.